Metallomics

PAPER

View Article Online
View Journal | View Issue

Cite this: *Metallomics*, 2019, 11, 799

Investigation of the calcium-induced activation of the bacteriophage T5 peptidoglycan hydrolase promoting host cell lysis†

Angelina O. Kovalenko,[a] Sergei V. Chernyshov,[a] Victor P. Kutyshenko,[b] Nikolai V. Molochkov,[b] Dmitry A. Prokhorov,[b] Irina V. Odinokova[b] and Galina V. Mikoulinskaia*[a]

Peptidoglycan hydrolase of bacteriophage T5 (EndoT5) is a Ca^{2+}-dependent L-alanyl-D-glutamate peptidase, although the mode of Ca^{2+} binding and its physiological significance remain obscure. Site-directed mutagenesis was used to elucidate the role of the polar amino acids of the mobile loop of EndoT5 (111–130) in Ca^{2+} binding. The mutant proteins were purified to electrophoretic homogeneity, the overall structures were characterized by circular dichroism, and the calcium dissociation constants were determined *via* NMR spectroscopy. The data suggest that polar amino acids D113, N115, and S117 of EndoT5 are involved in the coordination of calcium ions by forming the core of the EF-like Ca^{2+}-binding loop while the charged residues D122 and E123 of EndoT5 contribute to maintaining the loop net charge density. The results suggest that Ca^{2+} binding to the EndoT5 molecule could be essential for the stabilization of the long mobile loop in the catalytically active "open" conformation. The possible mechanism of Ca^{2+} regulation of EndoT5 activity during bacteriophage T5's life cycle through the Ca^{2+} concentration difference between the cytoplasm and the periplasm of the host bacteria cell has been discussed. The study reveals valuable insight into the role of calcium in the regulation of phage-induced bacterial lysis.

Received 31st January 2019,
Accepted 6th March 2019

DOI: 10.1039/c9mt00020h

rsc.li/metallomics

Significance to metallomics

The current research is the first attempt to incorporate calcium into a model of phage-mediated host cell lysis. To release phage progeny, bacteriophage T5 induces several proteins including calcium-dependent endolysin (EndoT5). The enzyme in the active site contains tightly bound catalytic zinc, and the role of loosely bound calcium, as well as the way of its binding, are unknown. This paper describes the study of calcium binding to EndoT5 by site-directed mutagenesis. The data obtained allowed the conclusion to be drawn that calcium activated EndoT5 in the periplasm of the bacteria, thereby promoting host cell lysis and progeny escape.

Introduction

Bacteriophage T5 requires calcium ions at different stages of its life cycle. Ca^{2+} is essential for the adsorption of a phage particle on the host cell surface as well as the maintenance of transcription and translation processes.[1–3] Endolysin of bacteriophage T5 (EndoT5) hydrolyzes peptidoglycan of the cell wall to cause cell lysis with subsequent release of phage progeny at the last stage of the phage's life cycle. As we have shown earlier, EndoT5 is regulated by Ca^{2+} ions which could be replaced by Mn^{2+} ions *in vitro*.[4]

EndoT5 is a small (137 amino acid residues) zinc-containing L-alanyl-D-glutamate peptidase related to the C subfamily of the M15 family.[5] Recently, the spatial solution structure of this protein in the presence of Zn^{2+} was characterized by high-resolution NMR spectroscopy (PDB ID: 2MZX).[6] EndoT5 represents a globular protein of the α + β class with the hydrophobic core

[a] *Branch of Shemyakin & Ovchinnikov's Institute of Bioorganic Chemistry RAS, Prospekt Nauki, 6, Pushchino, Moscow region 142290, Russia. E-mail: mikulinskaya@bibch.ru; Fax: +7-4967-330527; Tel: +7-4967-330527*

[b] *Institute of Theoretical and Experimental Biophysics RAS, Institutskaya ul., 3, Pushchino, Moscow region 142290, Russia*

† Electronic supplementary information (ESI) available: Table S1. List of the oligonucleotide primers used for site-directed mutagenesis. Red color indicates the introduced mutant nucleotide. F – forward primers and r – reverse primers. Fig. S1. (a) SDS-PAGE analysis of the mutant S117A/D122A preparations at the different purification steps. 1 – molecular weight markers (top down 116, 66.2, 45, 35, 25, 18.4, and 14.4 kDa), 2 – a crude extract, 3 – chromatography on the DEAE-Toyopearl 650M column, 4 – chromatography using phosphocellulose. The amount of protein applied was 5 μg per track. (b) Purified preparations of nine EndoT5 mutants. Fig. S2. Effect of exogenous Ca^{2+} on the activities of EndoT5 and its mutants. Types of mutants are indicated in boxes. Measurements were performed in triplicate, and results are presented as mean values ± SD. Fig. S3. Bacteriolytic effect of EndoT5 and its mutant E123A on living cells of stationary cultures of *P. aeruginosa* PAO1 with or without EDTA. Types of the enzymes are indicated in the box. Measurements were performed in triplicate, and results are presented as mean values ± SD. See DOI: 10.1039/c9mt00020h

composed of three α-helices and four antiparallel β-strands forming the β-sheet. The Zn^{2+} ion is coordinated in the enzyme structure by conserved amino acid residues H66, D73 and H133. The structure of EndoT5 was also shown to comprise a relatively long flexible disordered loop formed by residues 111–130, capable of binding paramagnetic ions.

The protein-bound Ca^{2+} ion is usually coordinated by 6–8 coordination bonds.[7] Oxygen atoms of side groups of Asp and Glu or their amides or the residues with hydroxyl groups in the side chain (Ser and Thr) are the most common ligands, thus oxygen atoms of peptide bonds and water molecules could also be involved.[8,9] The mobile loop 111–130 of EndoT5 is rich in polar residues (D113, N115, S117, D122, E123, and D130). The objectives of this study were to carry out site-directed mutagenesis of the polar residues of the EndoT5 flexible loop and assess the effect of single residue substitutions on Ca^{2+} binding, the enzyme activity, the secondary structure and the thermal resistance of EndoT5. The data obtained can give a glimpse into the regulatory mechanism of lysis timing in bacteriophage T5's life cycle.

Materials and methods

Bacteria strains, plasmids and chemicals

The following *E. coli* strains obtained from the All-Russian Collection of Microorganisms (IBPM RAS) were used: XL1Blue for the amplification of plasmids, BL21(DE3) and C41(DE3) for protein expression, and B (wild type) for analytical studies. Strain *P. aeruginosa* PAO1 was used for the analysis of the bacteriolytic action of the E123A enzyme. Bacteria were grown either in liquid LB broth or on agarized LB media. Media for the producing strains bearing the target plasmids contained 100 μg ml^{-1} of ampicillin.

The previously obtained recombinant plasmid pT5lys[4] constructed on the basis of the pET3a vector (Novagen, USA) and containing the *lys* gene encoding bacteriophage T5 endolysin was used as a template for site-directed mutagenesis. Synthesis of primers for mutagenesis was carried out by ZAO Evrogen (Russia). Sequences of primers are given in Table S1 (ESI†).

Most of the reagents used were purchased from Amresco (USA). For site-directed mutagenesis PfuUltra II DNA polymerase (Stratagene, USA) and Dpn I restriction endonuclease (Fermentas, Lithuania) were used. IPTG (Sigma, USA) was used to induce the synthesis of the target protein. For chromatography Toyopearl DEAE-650M (Tosoh, Japan) and phosphocellulose (Whatman, United Kingdom) were used.

Site-directed mutagenesis

Site-directed mutagenesis was performed using the QuikChange method developed by Stratagene (USA) (QuikChange® II XL Site-Directed Mutagenesis Kit, 2007). Amplification of the entire plasmid was performed using a high-precision thermostable DNA polymerase, PfuUltra II. After the PCR was complete, the mixture was digested using Dpn I restriction endonuclease to remove the methylated template plasmid DNA. Electroporation was carried out at a field intensity of 18 kV cm^{-1}. The pulse duration time averaged at 5.5 ms. The presence of the target mutation in the selected clones was validated by sequencing the corresponding site of the *lys* gene.

Isolation and purification of EndoT5 and mutants

Induction of EndoT5 and mutant synthesis was carried out in *E. coli* BL21(DE3)/*E. coli* C41(DE3) cells containing mutant variants of the plasmid. A colony of fresh *E. coli* transformants was transferred to a flask containing 250 ml of LB medium with ampicillin and grown at 37 °C, with the cell suspension stirred at 180 rpm until it reached the value of an optical density of 1 OD at 550 nm. Then IPTG was added to the cell culture at a concentration of 0.2 mM and the biomass was grown for another 3 hours (37 °C). The cells were collected by centrifugation at 5000*g* for 10 min. Chromatographic purification of proteins was carried out as described.[4] The fractions were analyzed by denaturing electrophoresis in 15% polyacrylamide gel using the Laemmli method.[10] Electrophoresis was carried out for 1.0–1.5 h at room temperature (field intensity, 15 V cm^{-1}). Gels were fixed in 10% trichloroacetic acid, stained with Coomassie Brilliant Blue G-250 (0.04% Coomassie G-250, 3.5% $HClO_4$) and washed with distilled water. The protein concentration in homogeneous preparations was determined spectrophotometrically from the absorbance at 280 nm, based on the molar extinction coefficient of the target protein.

Enzyme activity assay

Enzyme activity was determined using a spectrophotometric method based on a decrease in the optical density of a suspension of *E. coli* B cells preliminary permeabilized with chloroform. The measurements were carried out on a UV-1800 spectrophotometer (Shimadzu, Japan) at a wavelength of 450 nm and an optical density of 1 OD cells in a buffer (25 mM Tris/HCl (pH 8.0), 0.1% Triton-X100). The reaction was initiated by the addition of the enzyme. An activity unit was defined as the quantity of the enzyme that causes a decrease in the rate of optical density of 1.0 optical unit min^{-1}. All activity data were calculated from 3 independent measurements.

Evaluation of thermal resistance

Samples of the enzyme preparation – 100 μl of the protein solution in the storage buffer (25 mM Tris/HCl, 200 mM NaCl and 1 mM EDTA; pH 8.0) – were incubated in a solid state thermostat (DNA-Technology, Russia) at different temperatures (50, 70 and 90 °C) for 5, 10 and 30 min. After the incubation, the samples were cooled on ice for 10 min and assayed for the enzyme activity. The control samples were incubated for the same time on ice.

Measurement of circular dichroism spectra

Spectra of circular dichroism (CD spectra) in the far UV region (250–190 nm) were recorded using a JASCO J-810 spectropolarimeter with a thermostated cell (Jasco, Japan). The measurements were performed in 1 mm cuvettes; the concentration of protein in the samples was 10 nM. After the subtraction of the

buffer baseline, the spectra obtained were converted into molar ellipticity ([θ]) according to the following formula:

$$[\theta] = \frac{\text{data} \cdot M_r}{l \cdot c}$$

where [θ] is the molar ellipticity, deg cm^2 dmol^{-1}; data is the data from the spectropolarimeter, mdeg; M_r is the average molar mass of a single amino acid residue (g mol^{-1}); l is the optical length, mm; c is the concentration of the protein, mg ml^{-1}.

Changes in the secondary structure of the D130A mutant upon heating were studied by recording the CD spectra at 20 °C and 90 °C. After heating at 90 °C the sample was cooled to 20 °C for 30 minutes and the spectrum was recorded again.

Measurements of the effect of Ca^{2+} and EDTA on enzyme activity

To assess the effects of Ca^{2+} and EDTA, the activity of EndoT5 mutants was measured in the presence of 0.025, 0.05, 0.5 and 5 mM $CaCl_2$ or 0.06, 0.08, 0.1, 0.2, 0.5, 1, 2.5 and 3 mM EDTA, respectively. To assess the extent of enzymatic activity restoration, the mutants were incubated with EDTA in inhibitory concentrations of 0.1 mM (N115D and S117A) or 1 mM (D113A, N115A, D122A, E123A, S117A/D122A, and S117A/E123A). 0.02–0.04 units of the active enzyme were added to EDTA-containing medium. Then aqueous $CaCl_2$ was added and the activity was measured.

Bacteriolytic effect of the E123A mutant

1.0 OD (λ = 450 nm) of the *P. aeruginosa* night culture was precipitated by centrifugation at 5000*g* for 3 min, and the pellet was suspended in 1 ml of 25 mM Tris/HCl (pH 8.0). EDTA was added to a final concentration of 250 μM, and then the rate of cell lysis was measured spectrophotometrically. The reaction was initiated by the addition of an enzyme, either native EndoT5 or mutant E123A (0.05–0.2 active units).

NMR spectroscopy

NMR measurements were conducted on an AVANCE 600 III spectrometer with an operating frequency of 600 MHz, at 298 K, and a spectral width of 24 ppm and a 90 degree pulse of 11 μs. To calculate the dissociation constants, the ion-deprived lyophilized protein preparations were dissolved at a concentration of 2 mg ml^{-1}, dialyzed against 50 mM acetate buffer (pH = 4.2), and then saturated with zinc ions by the addition of $ZnCl_2$ solution. Saturation was controlled using NMR spectra; saturation was achieved at [Zn^{2+}] = 0.2 mM. Zinc-rich protein preparations were dialyzed against 50 mM acetate buffers with different pH values. The zinc-containing forms of the protein were titrated with Ca^{2+} by the addition of $CaCl_2$, while detecting changes in the proton signals in the up-field part of the spectrum. The equilibrium dissociation constants were calculated using the straight lines plotted in the Scatchard coordinates according to the equation:

$$\frac{1}{K}R_0 - \frac{1}{K}[\text{LR}] = \frac{[\text{LR}]}{L}$$

where K is the dissociation constant of the complex; L is the concentration of free calcium; [LR] is the concentration of the complex; R_0 is the initial concentration of the protein.

Software and statistical data processing

The design of the primers for site-directed mutagenesis was carried out using the Oligo4 program (USA). Interpretation of CD spectra was carried out using a software package for the analysis of protein spectra, CD–CDPro.[11] For the analysis of homologous amino acid sequences, we used the BLAST Search program[12] from the server of the National Center of Biotechnology Information (the National Library of Medicine, USA; http://www.ncbi.nlm.nih.gov/blast/). Multiple alignment of the amino acids was performed using the Clustal W program;[13] https://embnet.vital-it.ch/software/ClustalW.html. The consensus figure was generated using ESPript;[14] http://espript.ibcp.fr/ESPript/cgi-bin/ESPript.cgi. The statistical processing of the results was carried out using SigmaPlot 11.0 (Systat Software, Inc., 2008). The diagrams and tables show the mean values and their standard deviations. All measurements were carried out in triplicate.

Results

Site-directed mutagenesis

To elucidate the role of individual amino acid residues of EndoT5 in coordinating Ca^{2+} ions, polar residues D113, N115, S117, D122, E123, and D130 were selected, located in the enzyme mobile loop region. The conserved residue D130 for the proteins of the M15_C family, a constituent of the active site, was chosen as a reference since the mutant for this residue should not have either enzymatic activity or any alterations in Ca^{2+} binding. In all cases substitution with Ala was made. Alanine lacks the unusual backbone dihedral angle preferences and could not introduce conformational flexibility to the protein backbone. Substitution with Ala removes all side chain atoms past the β-carbon. Thus, the role of the side chain functional groups at specific positions can be inferred from Ala mutations.[15] Along with studying the effect of single mutations, the impact of the loop total charge density on catalysis was examined. For this purpose, the N115D mutant with an additional negative charge and two double mutants S117A/D122A and S117A/E123A with a significantly lower loop charge in comparison with the native enzyme were designed. Thus, we have obtained nine mutant proteins, namely, D113A, N115A, N115D, S117A, D122A, E123A, D130A, S117A/D122A, and S117A/E123A.

All mutant proteins were soluble and synthesized in the cytoplasm of producing strain cells with high efficiency. All proteins were purified to electrophoretic homogeneity and enzymatic purity using chromatographic methods with a high yield (70% or more). The purified preparations are shown in Fig. S1 (ESI†).

Control of the mutant protein structure

Circular dichroism (CD) spectra of native EndoT5 and mutant proteins (see Fig. 1a) showed that single residue substitutions do not lead to any significant change in the secondary structure

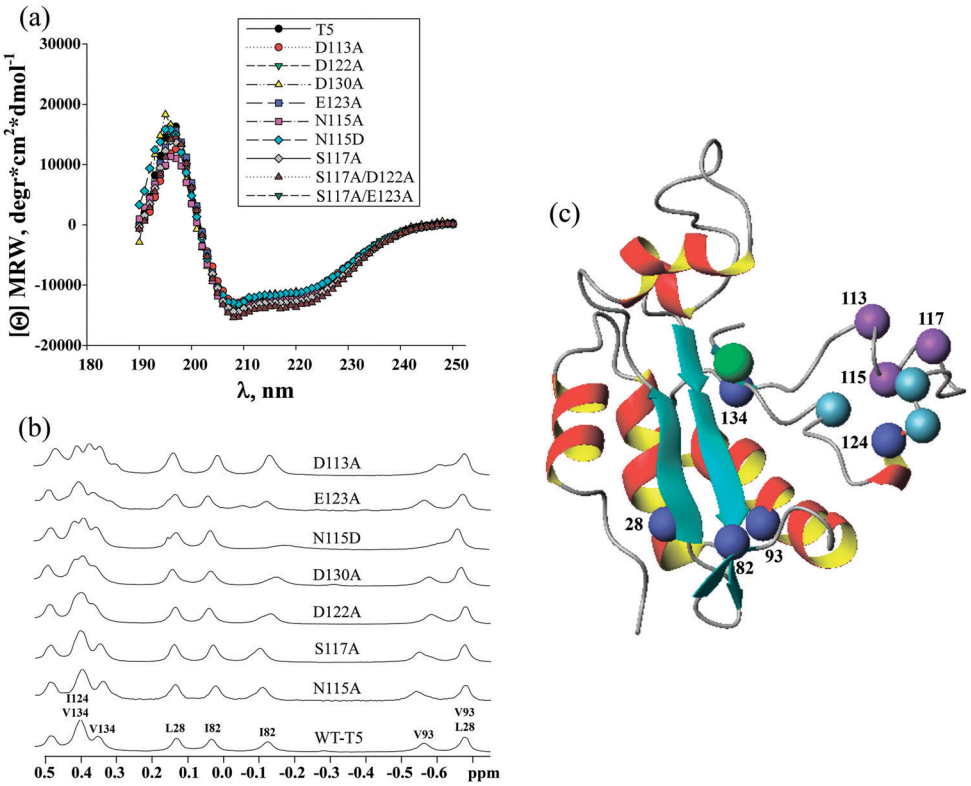

Fig. 1 (a) Far-UV circular dichroism spectra of wild-type EndoT5 and its mutants. Types of mutants are indicated in the box. Spectra were recorded in 1 mm cuvettes; the concentration of protein in the samples was 10 nM. (b) Up-field region of the ^{1}H-NMR spectra of EndoT5 and its mutants undergoing single substitutions measured in the presence of Zn^{2+} at pH 4.1 and T = 298 K. (c) Spatial localization of amino acid substitutions and structural responses. Amino acid numbers are indicated, the zinc atom is shown in green and single amino acid substitutions in the flexible loop are shown in purple and sky blue. Single-residue mutations which induce local structural perturbations are highlighted in deep blue.

of the designed mutants. The same is true for S117A/D122A and S117A/E123A double mutants. Calculation of the α-helical and β-fold content showed similar values of 26 ± 2% for α-helices and 25 ± 1% for β-fold structures in all preparations. Therefore, changes in the biochemical properties of mutant proteins with respect to wild-type EndoT5 are directly related to the functional role of mutated residues.

Fig. 1b represents the fragments of NMR spectra of mutant proteins arranged in descending order according to the similarity with native EndoT5. The up-field spectra area demonstrates some differences between the mutants and the native protein, indicating a subtle change in the system of intramolecular interactions. The local environmental disturbances induced by the single-residue mutations are depicted in Fig. 1c. As is shown, most of the amino acid residues whose environment is perturbed in response to the introduced mutations are localized in the hydrophobic core of the molecule. The exceptions include I124 located in the Ca-binding loop and I82 located in the β-turn.

N115A and S117A mutations without changing the charge within the Ca^{2+}-binding loop did not lead to any notable changes in the loop conformation or alterations in the environment of the loop I124 residue. The positions of the resonances of L28, V93 and V134 core residues also remained unaltered implying that the packing of the hydrophobic core of the molecule was preserved. D113A, N115D, and D122A mutations with a change in charge within the Ca^{2+}-binding loop caused significant alterations in the loop conformation and apparent restructuring in the packing of the protein hydrophobic core. The most pronounced disturbances of the loop were observed in the case of D113A and E123A replacements. However, the E123A replacement had virtually no effect on the packing mode of the hydrophobic core of the molecule. The introduction of an additional negative charge by N115D replacement was accompanied by changes in both the conformation of the Ca^{2+}-binding loop and the hydrophobic core packing. D122A and D130A substitutions have a significantly weaker but still detectible effect on the loop conformation as well as the core packing. In general, D113A, N115D, D122A, and E123A mutants with the changed loop charge exhibit the most prominent differences, which appear to be negligible for N115A and S117A mutants without charge loss and for the catalytic D130A mutant.

Effect of mutations on the enzyme activity

The value of specific activity is the most direct criterion of the mutations' impact on enzymatic catalysis. Table 1 shows the specific activities of mutant proteins in comparison with native EndoT5. The most pronounced effect on activity was obtained due to the substitution of Asp at position 113 since the D113A mutant has only residual activity, three orders of magnitude

Table 1 Specific activity values for wild-type EndoT5 and mutant proteins. Measurements were performed in triplicate, and results are presented as mean values ± SD. ND – activity is not determined

Enzyme	Specific activity, U mg^{-1}
EndoT5	8380 ± 140
D113A	6.5 ± 1.3
N115A	357 ± 33
N115D	2240 ± 202
S117A	265 ± 25
D122A	251 ± 23
E123A	837 ± 88
S117A/D122A	166 ± 0
S117A/E123A	256 ± 13
D130A	ND

lower than that of native EndoT5. The specific activity level of N115A, S117A, and D122A mutants was 25–35-fold lower than that of EndoT5. Both double mutants also demonstrated very low levels of activity (50- and 35-fold decrease for S117A/D122A and S117A/E123A, respectively). However, the E123A mutant remained relatively active, showing an activity of only an order of magnitude lower than that of EndoT5. Insertion of additional charge to position 115 also helped retain the activity at a sufficiently high level: the N115D mutant showed 25% of native protein activity. Finally, the D130A mutant completely lost enzymatic activity. We anticipated this result because this residue is conserved in zinc-containing peptidases of the M15_C family and is most likely directly involved in the process of nucleophilic substitution taking place during catalysis.

Effect of mutations on the thermal resistance

Native EndoT5 exhibits high thermal resistance as evidenced by convenient renaturation of its secondary structure and restoration of enzyme activity after heating.[16] Testing the thermal resistance of eight active mutants revealed that it was maintained at a level comparable with that of native EndoT5, demonstrating up to 65% of the initial activity restoration after a 30 min heating at 90 °C (Fig. 2a). To study the thermal resistance of the inactive D130A mutant, CD spectra were used. Fig. 2b shows CD spectra of the D130A mutant before, during and after a 10 min heating to 90 °C, respectively. The similarity of spectra before and after the heating indicates that the secondary structure of this inactive mutant was almost completely restored.

The D130A mutant retains the ability to bind the substrate

Interestingly, an excess of the D130A mutant in the reaction mixture prevents native EndoT5 from displaying its activity (see Fig. 3). This phenomenon cannot be explained by the aggregation of the active protein with an inactive mutant, since EndoT5 begins to associate at a concentration of 130 μM, which is two orders of magnitude greater than the maximum concentration used in this experiment (1.2 μM). Evidently, the inactive D130A mutant retains its ability to bind the substrate. Bovine serum albumin used as a negative control did not affect the activity of the native enzyme even when added in a 100-fold excess.

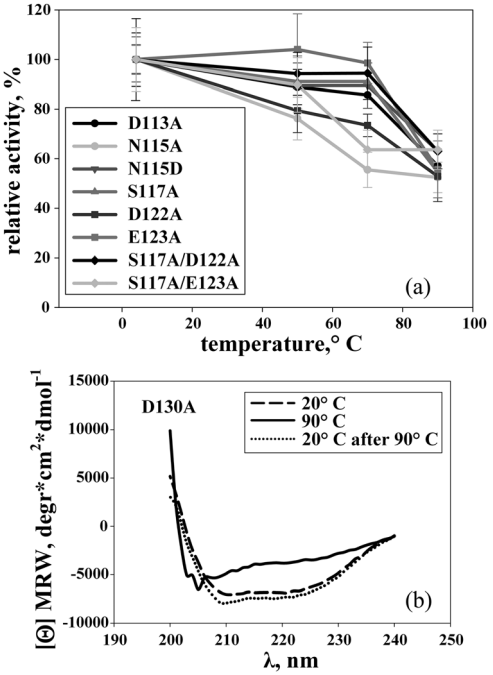

Fig. 2 Thermal resistance of EndoT5 and its mutants. (a) Relative activity of mutant proteins after incubation at different temperatures for 30 min. Relative activity units are given as percentage values relative to initial sample activities defined as 100%. Measurements were performed in triplicate. Results are stated as mean values ± SD. (b) Far-UV CD spectra of fully inactive mutant EndoT5D130A at 20 °C before heating (long dashed lines), at 90 °C (solid lines), and at 20 °C after heating (dotted lines).

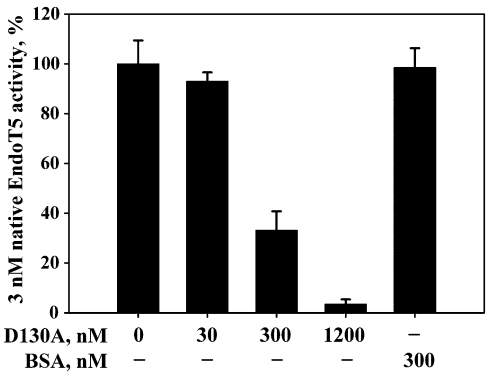

Fig. 3 Effect of mutant D130A added to the reaction medium on the activity of native EndoT5. Activity of EndoT5 without D130A defined as 100%. Measurements were performed in triplicate. Results are stated as mean values ± SD.

Effect of calcium and EDTA on enzyme activity

As with the native enzyme, an excess of Ca^{2+} in the reaction mixture leads to the inhibition of the mutant protein activity at concentrations of 0.5 mM and above (the data are illustrated in Fig. S2 of the ESI†). Obviously, this inhibition is nonspecific. Only the S117A mutant demonstrates small activation at this concentration of Ca^{2+}. This could arise from reduced affinity for Ca^{2+} and an increased dissociation constant as compared with the native protein.

The activity of native EndoT5 was previously shown not to be inhibited by zinc-specific chelating agent 1,10-phenanthroline.[4] NMR spectra testify to high binding affinity of the zinc ion within a protein at physiological pH values.[6] However, a broad-spectrum chelator, EDTA, and a calcium-specific chelator, BAPTA, inhibit EndoT5 activity at an equal concentration of 60 μM due to the removal of Ca^{2+} from the medium since the addition of Ca^{2+} fully restores the enzyme activity in both cases.[4]

The mutants could be divided into three groups based on the inhibitory effect of EDTA on their activity (Fig. 4a–c). EDTA at a concentration of 60 μM completely inhibits the activity of N115D and S117A (group 1) as in the case of native EndoT5. Full inhibition of D113A and N115A (group 2) requires higher concentrations of chelator (0.1–0.5 mM). As for D122A, E123A and the double mutants S117A/D122A and S117A/E123A (group 3), 1 mM of EDTA is not sufficient to inhibit their activity completely: they still retain residual activity even at 3 mM of EDTA.

Three groups of mutants differ in the activity restoration extent after inhibition by EDTA (Fig. 4d–f). The mutants of group 1 like wild-type EndoT5 fully restored their activity. The mutants of group 3 restored more than half of their activity whereas Ca^{2+}-dependent restoration of activity for the mutants of group 2 did not exceed 20% indicating that the Ca^{2+} coordination was severely impaired for these mutants.

The data on the inhibition of the activity of the enzymes by EDTA in experiments on D113A and S117A mutants were confirmed using Ca^{2+}-specific chelator BAPTA; the results for both inhibition and activity recovery by calcium were identical.

Residues 113–123 form EF-like loops

The consensus amino acid sequence of the canonical 12-residue Ca^{2+}-binding EF-loop starts with Asp and ends with a Glu residue (Fig. 5a). The EF-loop provides 6 ligands for Ca^{2+} coordination located at positions 1, 3, 5, 7, 9 and 12 (they are

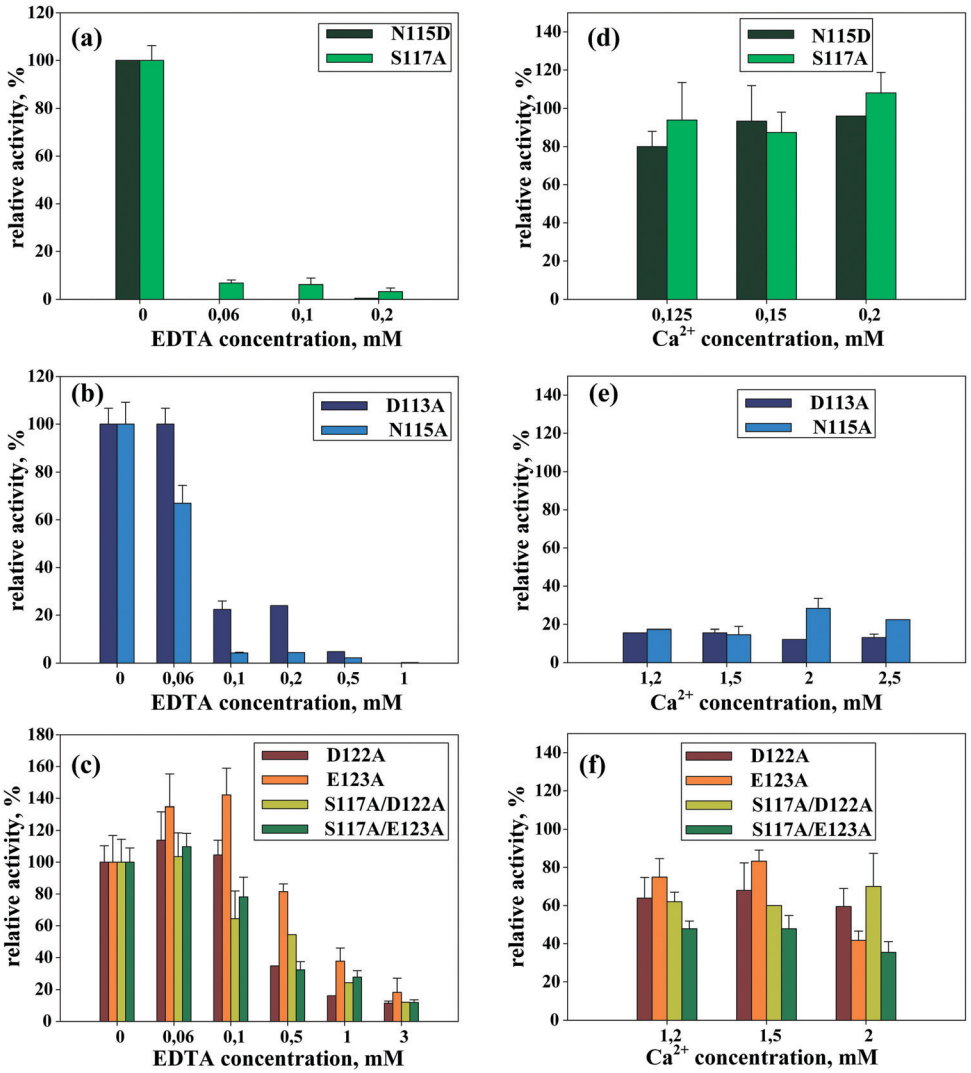

Fig. 4 Effect of Ca^{2+} and EDTA on the activities of EndoT5 and its mutants. Types of mutants are indicated in the boxes. (a–c) Inhibition of activity in three groups of mutants by EDTA added in low (for N115D and S117A, A), medium (for N115A and D113A, B) and high (for D122A, E123A, S117A/D122A and S117A/E123A, C) concentrations. (d–f) Activity recovering in three groups of mutants by Ca^{2+} added after inhibition by EDTA. Relative activity units are given as percentage values relative to a maximal activity without a chelator or Ca^{2+} defined as 100%. Measurements were performed in triplicate. Results are stated as mean values ± SD.

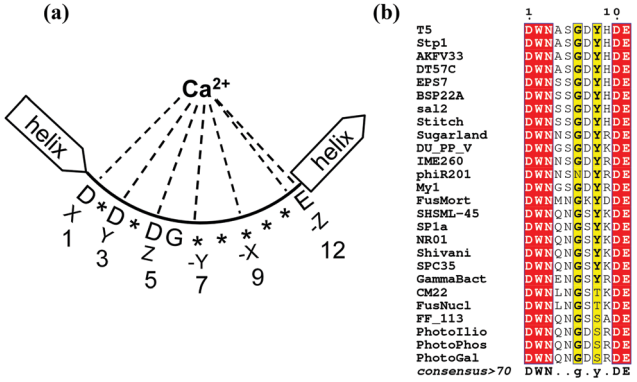

Fig. 5 Calcium-binding motifs of EF-type proteins. (a) "Canonical" EF-loop and its consensus sequence. The direction of incoming and exiting helices is indicated by the pointed end of the box. The dashed lines denote the coordination bonds and letters *X*, *Y*, *Z*, −*X*, −*Y*, −*Z* are ligands that form them. The numbers indicate the ligand positions relative to the beginning of the loop. (b) Sequence alignment of the 11-residue calcium-binding site of EndoT5 and homologous peptidases. Abbreviations denote proteins of the following sources (GenBank accession numbers are given in brackets): T5 – bacteriophage T5 (YP_006868.1); Stp1 – *Salmonella* phage Stp1 (ARQ96246.1); AKFV33 – *Escherichia* virus AKFV33 (YP_006382340.1); DT57C – *Escherichia* virus DT57C (YP_009149816.1); EPS7 – *Escherichia* virus EPS7 (YP_001836966.1); BSP22A – *Salmonella* phage BSP22A (ARM69709.1); sal2 – *Salmonella* phage 100268_sal2 (YP_009320767.1); Stitch – *Salmonella* virus Stitch (YP_009145980.1); Sugarland – *Klebsiella* phage Sugarland (ATW61880.1); DU_PP_V – *Pectobacterium* phage DU_PP_V (ATS94012.1); IME260 – *Klebsiella* phage vB_Kpn_IME260 (APT41082.1); phiR201 – *Yersinia* phage phiR201 (YP_007237012.1); My1 – *Pectobacterium* phage My1 (YP_006906290.1); FusMort – *Fusobacterium mortiferum* (WP_005885324.1); SHSML-45 – *Shigella* phage SHSML-45 (YP_009280248.1); SP1a – *Salmonella* phage SP1a (ATI18557.1); NR01 – *Salmonella* phage NR01 (YP_009283472.1); Shivani – *Salmonella* phage Shivani (YP_009194685.1); SPC35 – *Salmonella* virus SPC35 (YP_004306522.1); GammaBact – *Gammaproteobacteria bacterium* (PID66617.1); CM22 – *Fusobacterium* sp. CM22 (WP_032845865.1); FusNucl – *Fusobacterium nucleatum* (WP_008701476.1); FF_113 – *Enterovibrio* sp. FF_113 (AKN38799.1); PhotoIlio – *Photobacterium iliopiscarium* (WP_052675216.1); PhotoPhos – *Photobacterium phosphoreum* (WP_107197689.1); PhotoGal – *Photobacterium galatheae* (WP_036748994.1).

denoted by *X*, *Y*, *Z*, −*Y*, −*X*, −*Z*, where *X* is the first, and *Z* is the last ligand).[17] The first 6 positions of the canonical EF-loop have a consensus sequence DxDxDG.[18] At position 7 (−*Y*), the carbonyl oxygen atom of the peptide bond of the less conserved residue is located. Residue E at position 12 of the loop donates two oxygen atoms of its γ-carboxyl group for Ca^{2+} binding, acting as a bidentate ligand. Thus, in most EF-hand proteins, 7 oxygen atoms organized in a pentagonal bipyramid coordinate the Ca^{2+} ion.

The sequence of residues from 113 to 123 of EndoT5 (Fig. 5b) features a pronounced similarity to the EF-loop since conserved polar residues D113, N115 and S117 could be attributed to *X*, *Y* and *Z* ligands and G118 fits into the 6th position of the loop consensus sequence. However, neither the sequence of the C-terminal part of the loop (D122 and E123) nor the length (11 amino acid residues) corresponds to the canonical EF-loop, thus suggesting an EF-like Ca^{2+} binding.

Sequences homologous to such truncated EF-loops are found in a number of phages infecting *Escherichia coli* or related bacteria species such as *Klebsiella*, *Salmonella*, and *Yersinia* (Fig. 5b). Some of these sequences have a bacterial prophage origin. Nevertheless, the length and homology of whole proteins suggest that all of them belong to proteases of the M15 family. The amino acid consensus sequence as shown in Fig. 5b is highly conserved, but the prediction of the secondary structure using JPred (http://www.compbio.dundee.ac.uk/jpred4/index_up.html),[19] does not reveal any regularity in this area. This is consistent with the evidence obtained from the study of the EndoT5 spatial structure, showing that this region is disordered and represents a flexible loop in the absence of Ca^{2+}.[6]

Ca^{2+} dissociation constants of EndoT5 mutants

NMR spectroscopy was used to measure Ca^{2+} dissociation constants (K_d) for native EndoT5 and mutants with single substitutions. Alterations in up-field signals were quantified when the protein was titrated with Ca^{2+} ions. The data obtained are summarized in Table 2. The study of full-length proteins *via* NMR spectroscopy is preferable in an acid medium since these conditions provide high-quality spectra. For five mutant proteins studied, the affinity for Ca^{2+} was reduced to such an extent that it was not possible to measure K_d under the selected conditions. However, constants were obtained for the native protein as well as for the D130A and N115D mutants. In the case of N115D, the Ca^{2+} affinity was reduced by an order of magnitude. The increase in the K_d value correlates with the decrease in enzymatic activity. The catalytic residue mutant (D130A) was completely inactive but still retained its Ca^{2+}-binding ability: K_d at pH 4.2 was close to that of native EndoT5.

Since the pH in the cell is higher than the optimal value for NMR spectroscopy (pH 4.2), K_d of the native protein was measured at different pH values. K_d at pH 6.2 was 0.21 ± 0.01 mM which slightly differs from the value obtained at pH 5.2, suggesting that this value is an adequate estimate of EndoT5 Ca^{2+} affinity.

Lysis of *Pseudomonas aeruginosa* cells by the E123A mutant

When examining the biochemical properties, we noticed that some EndoT5 mutants were resistant to high concentrations of

Table 2 Some parameters of Ca^{2+} binding for EndoT5 and its single residue mutants. Measurements were performed in triplicate, and results are presented as mean values ± SD. ND – constants were not determined

	pH	Binding constant *K*, mM^{-1}	Dissociation constant $K_d = 1/K$, mM	Titration step, mM	R^2
Endo T5	4.2	0.71 ± 0.03	1.41 ± 0.06	0.20	0.99
	5.2	4.43 ± 0.46	0.23 ± 0.03	0.05	0.95
	6.2	4.79 ± 0.18	0.21 ± 0.01	0.05	0.99
D130A	4.2	0.45 ± 0.01	2.22 ± 0.05	0.4	0.94
N115D	5.2	0.47 ± 0.04	2.11 ± 0.02	0.4	0.94
N115A, D113A, S117A, D122A, E123A	4.2	ND			

EDTA (Fig. 4c). Furthermore, the Glu-123 mutant exhibited sufficiently high lytic activity under these conditions. We tested the bacteriolytic activity of E123A on living cells of the laboratory strain *Pseudomonas aeruginosa* PAO1. In contrast to the native enzyme, the E123A mutant exhibited 200 units of specific activity on living cells of pseudomonas in the presence of 250 μM EDTA which permeabilized the outer membrane of *Pseudomonas* (Fig. S3, ESI†).

Discussion

Calcium is the fifth most abundant chemical element in the earth's crust.[20] In the ionized form, it is one of the most essential regulators of the processes occurring in living organisms at the cellular level. In eukaryotic cells, Ca^{2+} acts as a secondary messenger in signal transmission and binds a variety of proteins, changing their properties and functioning.[21,22] In bacteria, Ca^{2+} is involved in the regulation of cell division, mobility, chemotaxis, and transport.[18] Ca^{2+} is needed to maintain the integrity and stability of the bacterial cell wall and the external lipopolysaccharide layer of Gram-negative microorganisms.[23] Viruses, as obligate intracellular parasites, also develop smart strategies to manipulate the host Ca^{2+} to benefit their own life cycles.[20]

Studies on the process of Ca^{2+} and other cations binding to proteins usually include the measurement of enzymatic activity in an ion deficient medium, spectrofluorometric titration or CD in the near ultraviolet region. However, these methods are not applicable to bacteriophage T5 endolysin: (i) a substrate for activity measuring contains an excess of Ca^{2+}, (ii) all three EndoT5 tryptophan residues are exposed, so no shifts in the maximum fluorescence position can be detected, (iii) CD spectra do not reveal any changes in the absence of a regular secondary structure in the vicinity of the calcium-binding loop. To study Ca^{2+} regulation of EndoT5, we applied site-directed mutagenesis accompanied by biochemical analysis and measured Ca^{2+} dissociation constants for the native protein and a number of mutants. The obtained data allowed us to make certain conclusions about the role of individual amino acid residues of the flexible loop formed by residues 111–130 in Ca^{2+} regulation of EndoT5.

As in the case of the EndoT5 wild-type enzyme, the activity of N115D and S117A mutant proteins is easily inhibited by EDTA and subsequently restored by the addition of Ca^{2+}. This suggests that both mutant proteins retain the specificity of Ca^{2+} binding, although with a lower affinity. The reduced activity of the N115D mutant accompanied by an increase in the dissociation constant could arise from the introduction of an additional negative charge. Interestingly, changes in the charge of calmodulin Ca^{2+}-binding loops showed that the addition of the sixth acidic chelating residue to Ca^{2+}-binding sites reduced the Ca^{2+} affinity.[24] Noteworthily there is a considerable loss of the S117A mutant activity. This is clear evidence that Ser-117 is involved in the coordination of the Ca^{2+} ion.

D113A and N115A mutant proteins display low activity and their inhibition by EDTA is almost irreversible. Therefore, residues in positions 113 and 115 are essential for ensuring both the strength and the specificity of Ca^{2+} binding and are directly involved in the coordination of the ion. Asp in position 113 is of particular importance since the D113A mutant has only residual activity.

Mutant proteins D122A and E123A, as well as double mutants S117A/D122A and S117A/E123A, have reduced activity and are inhibited by high concentrations of EDTA. The activity of these mutants is almost completely restored by Ca^{2+} ions. The specificity of Ca^{2+} binding is most likely retained, implying that Asp in position 122 and Glu in position 123 could provide the required charge density.

The increase in chelator concentrations required to inhibit the activity of Ala mutants lacking polarity (these include D113A, N115A, D122A, E123A and double mutants) may be a consequence of a change in the loop conformation due to reduced repulsion between similarly charged groups. Obviously, N115D and S117A mutants do not lose charge. Enhanced resistance to EDTA along with a sufficient level of specific activity makes the E123A mutant a promising candidate for application as an antibacterial agent against *Pseudomonas*. Unlike membranes of *Enterobacteria* cells which are resistant to EDTA up to 5 mM due to a low content of membrane phosphate groups,[25] cation-rich membranes of *Pseudomonas* are sensitive to EDTA and therefore susceptible to permeabilization by this chelator.[26] We have also shown the E123A mutant to demonstrate high lytic activity on living cells of a stationary *Pseudomonas* culture in the presence of 250 μM EDTA, whereas the native enzyme is inhibited under these conditions. Thus, the result of mutagenesis initially conducted for the purposes of fundamental research may have some practical potential.

Also worth considering is the mutation in position 130, leading to the complete loss of enzyme activity. Asp in this position constitutes the active center and seems pivotal for catalysis. The substitution of D130A does not significantly affect Ca^{2+} affinity. The fact that despite the total loss of activity the mutant for this residue retains the ability to bind the substrate suggests that EndoT5–peptidoglycan interaction is not connected with catalysis but involves other regions of this globular monomeric protein.

Residues D113, N115, and S117 resemble the N-terminal region of the loop of the EF-hand domain. EF-hand type domains (EF-hand), first discovered in the early 1970s,[27] are the most wide-spread calcium-binding motifs.[28] The canonical Ca^{2+}-binding EF-hand is composed of two α-helices, incoming and exiting, with a loop in between, where Ca^{2+} is coordinated by ligands at positions 1, 3, 5, 7, 9 and 12[29] (Fig. 5a). Non-canonical EF-hands differ from this template wherein they either lack the α-helix (incoming or exiting) or have deletions or insertions in the N-terminal region of the loop.[21] Some proteins have been shown to have a more compact EF-loop due to the presence of Asp at position 12;[30] another example of a non-canonical loop is represented by the so-called ''pseudo EF-hand'' loop (ψ-hand), which contains 14 residues.[17] There is also an 11-residue loop (calpain and grancalcin) along with a 13-residue loop (osteonectin).[22] All insertions and deletions are

usually localized in the variable N-terminal region of a loop whereas the C-terminal part has conserved its structure and length.[22] Another variant of Ca^{2+} binding is represented by the formation of an octahedral conformation instead of a pentagonal bipyramid.[31]

In the case of EndoT5, it is possible to speak of EF-like Ca^{2+} binding to a flexible loop formed by residues 113–123. The N-terminal region of this loop contains D113, N115, and S117 residues corresponding to positions 1, 3, and 5 of the canonical consensus sequence. The results of a mutagenesis study clearly demonstrate the importance of each residue for Ca^{2+} regulation. Mutants with substitution of polar residues for Ala at positions 113, 115, and 117 have a greatly reduced Ca^{2+} affinity and a very low enzymatic activity. Gly-118 is also a valuable element of the EF-hand domain providing the functionally significant turn of the polypeptide chain.[21] However, in the case of EndoT5, the C-terminal part of the loop has a shorter length and differs from the canonical version in residue composition. The loop is also not flanked with α-helices.[6] The last Glu of the canonical EF-hand loop plays a key role in providing bidentate binding.[29] In our case, mutant E123A was the most active one among other Ala mutants. We assume that C-terminal residues D122 and E123 are essential for maintaining the charge density, while the conserved polar residues D113, N115 and S117 constitute the core of the Ca^{2+}-binding loop. The consensus sequence DWNxxGxxxDE is inherent in a number of homologous EndoT5 peptidases belonging to the family of zinc-containing metallopeptidases M15 of predominantly phage origin (Fig. 5b).

In most eukaryotic proteins, EF-hand domains are paired but proteins with an odd number of EF-hand domains are known to exist.[7] Prokaryotic EF-hand containing proteins are less common and their Ca^{2+}-binding domains are usually unpaired.[18] EF-hand proteins are divided into two groups according to their Ca^{2+}-binding ability: Ca^{2+}-buffers and Ca^{2+}-sensors.[21] The buffers bind Ca^{2+} with an affinity of less than 100 nM and do not undergo any significant restructuring. The sensors bind Ca^{2+} with an affinity of 1–10 μM and Ca^{2+} induces considerable conformational changes in the structure of sensors enabling their interaction with other proteins to provide some important activity for the cell.[32] We believe that EndoT5 could nominally be classified as a sensor as Ca^{2+} produces a functionally significant effect on the EndoT5 molecule, involving a Ca^{2+}-dependent structural rearrangement to the catalytically active ''open'' conformation. This suggestion is indirectly confirmed by the analysis of the protein spatial structure in the Ca^{2+}-free state.[6] The disordered loop 113–123 is able to close the active center and thereby prevent catalysis.

Ca^{2+} can stabilize enzyme structures at high temperatures, *e.g.* of some metallopeptidases of the families M4, M7, and M10.[33] We showed that a decrease in the affinity for calcium caused by mutagenesis did not result in lower thermal resistance of EndoT5 mutants including double mutants. Thus, the thermal resistance of EndoT5 is not directly related to Ca^{2+} in contrast to that of thermostable thermolysin-like or subtilisin-like proteases.[34,35]

An example of phage-specific Ca^{2+}-binding endolysin containing the EF-hand domain is the LysGH15 enzyme of the GH15 staphylococcal phage (or the almost identical LysK homologue of staphylococcal phage K).[36,37] LysGH15 and LysK have a modular structure containing two catalytic (CHAP and Amidase-2) and one adsorption domain (SH3b). The structure of the CHAP domain of LysGH15 and LysK has been shown to comprise the canonical 12-residue Ca^{2+}-binding EF-loop (positions of ligands 1, 3, 5, 7 and 12) and one α-helix.[36,37] LysGH15 (or LysK) is the first example of a phage endolysin containing an EF hand-like motif in its structure. We have shown that EndoT5 also has an EF-like Ca^{2+}-binding loop that is substantially different from the canonical one. Interestingly, the CHAP domain of LysK also contains Zn^{2+}, which is more loosely bound and coordinated with the Cys residue (LysK is a cysteine protease).

Beyond discussions of the way Ca^{2+} binds EndoT5, a question arises about the biological utility of Ca^{2+} regulation of this phage-specific protein participating in the lysis of a bacterial cell. Considering the bound Zn^{2+} in the active center, could the presence of an additional ion and the corresponding complex regulation be an aggravating evolutionary circumstance limiting the phage's expansion or its yield? We don't think so.

Ca^{2+} dissociation constants (K_d) of EndoT5 are quite high if compared with, for example, recoverin (3.2 μM and 2.7 μM) for Ca^{2+}-binding sites II and III, respectively[9] or parvalbumin (10^{-8}–10^{-10} M).[38] Cytoplasmic Ca^{2+} concentration in bacterial cells is maintained at a low level of 100–300 nM.[18] Since the Ca^{2+} dissociation constant of EndoT5 measured under near-native conditions – 0.21 ± 0.01 mM – is three orders of magnitude higher, and endolysin synthesized in the cytoplasm of the infected cell would be inactive. However, the concentration of Ca^{2+} in the cell periplasm where the substrate of endolysin, peptidoglycan, is located, exceeds 100 μM and can reach 1 mM.[39] Obviously, the Ca^{2+} activation of EndoT5 takes place in the periplasm.

The lysis of a Gram-negative bacterial cell by a lytic bacteriophage is a complex process usually involving cooperation of four phage-specific proteins: endolysin degrades the peptidoglycan of the cell wall; holin provides access to the periplasm by forming the inner membrane pore, whose size depends on the type of holin,[40] and a couple of auxiliary phage proteins called i-spanin and o-spanin interact in the periplasm, providing the fusion of the inner and outer membranes at the final stage of lysis.[41] In bacteriophage T5, the genes of holin (AAX11974.1) and endolysin (AAS19387.1) are located in the early genome region in the same operon, while i-spanin (YP_006873.1) and o-spanin (YP_006872.1) are easily identified in the adjacent operon. Holin of bacteriophage T5 belongs to the T4 holin family having the N-terminal membrane domain and a large periplasmic domain and like other representatives of the T4 family holins are capable of forming large pores in the inner membrane.[42,43] Phage T5 i-spanin and o-spanin have a structural similarity (but not amino acid homology) with classical lambdoid-type spanins, although they are not coded by a common gene. i-Spanin has an N-terminal transmembrane

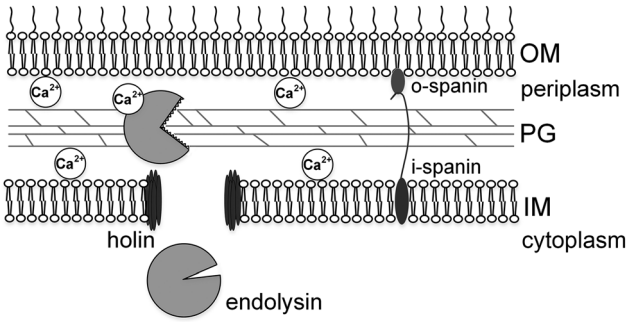

Fig. 6 Scheme of the cell wall lysis of *Escherichia coli* mediated by bacteriophage T5-induced lysis proteins – holin, Ca^{2+}-regulated endolysin and spanins. IM – inner membrane, OM – outer membrane, and PG – cross-linked peptidoglycan layer.

domain and o-spanin has a removable sec-type signal peptide and a site of lipoylation for anchoring to the outer membrane by a fatty acid residue. A schematic model of cell lysis by bacteriophage T5 involving Ca^{2+} regulation is shown in Fig. 6.

The lysis process of the cells infected with bacteriophage should occur at a precise scheduled time to provide an assembly and maturation of phage particles as well as their sufficient yield. Complex regulation of holins involves triggering the pore formation in the cell internal membrane when the proper moment for lysis approaches, which is why holin is generally recognized as the ''biological clock'' setting up the so-called lysis timing.[44,45] Endolysins can be synthesized in the cytoplasm over most of the phage life cycle since their genes often have early promoters. However, EndoT5, a peptidase with a high specific activity and capable of autocatalytic cleavage, cannot be non-toxic to other cytoplasmic proteins. For example, EndoRB43, another phage L,D-peptidase, which has no Ca^{2+} regulation but possesses high specific activity, is toxic to bacterial cells upon overproduction.[46] We consider periplasmic activation of EndoT5 by Ca^{2+} to be an evolutionary advantage that adds another regulation level to provide a higher phage yield and refine the activity network at the final stage of infection. Calcium therefore could represent the ''fifth element'' of the lysis process. Without Ca^{2+} tuning of endolysin the quartet of holin, endolysin, i-spanin and o-spanin appears to be a necessary but not sufficient tool for the carefully-choreographed lysis.

List of abbreviations

BAPTA	1,2-Bis-(*o*-aminophenoxy)ethane-*N*,*N*,*N*′,*N*′-tetraacetic acid
CD	Circular dichroism
Deg	Degree
EndoT5	Bacteriophage T5 endolysin
NMR	Nuclear magnetic resonance

Conflicts of interest

No conflict of interest declared.

Acknowledgements

This work was supported by the Russian Foundation for Basic Research (grant no. 18-04-00492).

References

1 M. Bonhivers and L. Letellier, Calcium controls phage T5 infection at the level of the Escherichia coli cytoplasmic membrane, *FEBS Lett.*, 1995, **374**, 169–173.
2 R. W. Moyer and J. M. Buchanan, Effect of calcium ions on synthesis of T5-specific ribonucleic acid, *J. Biol. Chem.*, 1970, **245**, 5904–5913.
3 R. W. Moyer and J. M. Buchanan, Effect of calcium ions on synthesis of T5-specific proteins, *J. Biol. Chem.*, 1970, **245**, 5897–5903.
4 G. V. Mikoulinskaia, I. V. Odinokova, A. A. Zimin, V. Y. Lysanskaya, S. A. Feofanov and O. A. Stepnaya, Identification and characterization of the metal ion-dependent L-alanoyl-D-glutamate peptidase encoded by bacteriophage T5, *FEBS J.*, 2009, **276**, 7329–7342.
5 G. V. Mikoulinskaia, I. V. Odinokova, A. A. Zimin and O. A. Stepnaya, L-Alanoyl-D-Glutamate Peptidase (Bacteriophage T5), *Handbook of Proteolytic Enzymes*, 3rd edn, 2013, vol. 1 and 2, pp. 1407–1410, DOI: 10.1016/B978-0-12-382219-2.00316-1.
6 D. A. Prokhorov, G. V. Mikoulinskaia, N. V. Molochkov, V. N. Uversky and V. P. Kutyshenko, High-resolution NMR structure of a Zn^{2+}-containing form of the bacteriophage T5 L-alanyl-D-glutamate peptidase, *RSC Adv.*, 2015, **5**, 41041–41049.
7 E. Carafoli and J. Krebs, Why Calcium? How Calcium Became the Best Communicator, *J. Biol. Chem.*, 2016, **291**, 20849–20857.
8 M. Kumar, S. Ahmad, E. Ahmad, M. A. Saifi and R. H. Khan, In silico prediction and analysis of Caenorhabditis EF-hand containing proteins, *PLoS One*, 2012, **7**, e36770.
9 S. E. Permyakov, A. M. Cherskaya, I. I. Senin, A. A. Zargarov, S. V. Shulga-Morskoy, A. M. Alekseev, D. V. Zinchenko, V. M. Lipkin, P. P. Philippov, V. N. Uversky and E. A. Permyakov, Effects of mutations in the calcium-binding sites of recoverin on its calcium affinity: evidence for successive filling of the calcium binding sites, *Protein Eng.*, 2000, **13**, 783–790.
10 U. K. Laemmli, Cleavage of structural proteins during the assembly of the head of bacteriophage T4, *Nature*, 1970, **227**, 680–685.
11 N. Sreerama and R. W. Woody, Estimation of protein secondary structure from circular dichroism spectra: comparison of CONTIN, SELCON, and CDSSTR methods with an expanded reference set, *Anal. Biochem.*, 2000, **287**, 252–260.
12 S. F. Altschul, T. L. Madden, A. A. Schaffer, J. Zhang, Z. Zhang, W. Miller and D. J. Lipman, Gapped BLAST and PSI-BLAST: a new generation of protein database search programs, *Nucleic Acids Res.*, 1997, **25**, 3389–3402.
13 M. A. Larkin, G. Blackshields, N. P. Brown, R. Chenna, P. A. McGettigan, H. McWilliam, F. Valentin, I. M. Wallace, A. Wilm, R. Lopez, J. D. Thompson, T. J. Gibson and D. G. Higgins, Clustal W and Clustal X version 2.0, *Bioinformatics*, 2007, **23**, 2947–2948.

14 X. Robert and P. Gouet, Deciphering key features in protein structures with the new ENDscript server, *Nucleic Acids Res.*, 2014, **42**, W320–W324.
15 K. L. Morrison and G. A. Weiss, Combinatorial alanine-scanning, *Curr. Opin. Chem. Biol.*, 2001, **5**, 302–307.
16 M. S. Shavrina, A. A. Zimin, N. V. Molochkov, S. V. Chernyshov, A. V. Machulin and G. V. Mikoulinskaia, *In vitro* study of the antibacterial effect of the bacteriophage T5 thermostable endolysin on Escherichia coli cells, *J. Appl. Microbiol.*, 2016, **121**, 1282–1290.
17 H. Kawasaki, S. Nakayama and R. H. Kretsinger, Classification and evolution of EF-hand proteins, *BioMetals*, 1998, **11**, 277–295.
18 D. C. Dominguez, M. Guragain and M. Patrauchan, Calcium binding proteins and calcium signaling in prokaryotes, *Cell Calcium*, 2015, **57**, 151–165.
19 A. Drozdetskiy, C. Cole, J. Procter and G. J. Barton, JPred4: a protein secondary structure prediction server, *Nucleic Acids Res.*, 2015, **43**, W389–W394.
20 Y. Zhou, S. Xue and J. J. Yang, Calciomics: integrative studies of Ca^{2+}-binding proteins and their interactomes in biological systems, *Metallomics*, 2013, **5**, 29–42.
21 J. L. Gifford, M. P. Walsh and H. J. Vogel, Structures and metal-ion-binding properties of the Ca^{2+}-binding helix-loop-helix EF-hand motifs, *Biochem. J.*, 2007, **405**, 199–221.
22 Z. Grabarek, Structural basis for diversity of the EF-hand calcium-binding proteins, *J. Mol. Biol.*, 2006, **359**, 509–525.
23 V. Norris, M. Chen, M. Goldberg, J. Voskuil, G. McGurk and I. B. Holland, Calcium in bacteria: a solution to which problem?, *Mol. Microbiol.*, 1991, **5**, 775–778.
24 D. J. Black, S. B. Tikunova, J. D. Johnson and J. P. Davis, Acid pairs increase the N-terminal Ca^{2+} affinity of CaM by increasing the rate of Ca^{2+} association, *Biochemistry*, 2000, **39**, 13831–13837.
25 H. Oliveira, V. Thiagarajan, M. Walmagh, S. Sillankorva, R. Lavigne, M. T. Neves-Petersen, L. D. Kluskens and J. Azeredo, A thermostable Salmonella phage endolysin, Lys68, with broad bactericidal properties against Gram-negative pathogens in presence of weak acids, *PLoS One*, 2014, **9**, e108376.
26 Y. Briers, M. Walmagh, V. Van Puyenbroeck, A. Cornelissen, W. Cenens, A. Aertsen, H. Oliveira, J. Azeredo, G. Verween, J. P. Pirnay, S. Miller, G. Volckaert and R. Lavigne, Engineered endolysin-based "Artilysins" to combat multidrug-resistant Gram-negative pathogens, *mBio*, 2014, **5**, e01379.
27 R. H. Kretsinger and C. E. Nockolds, Carp muscle calcium-binding protein. II. Structure determination and general description, *J. Biol. Chem.*, 1973, **248**, 3313–3326.
28 S. Henikoff, E. A. Greene, S. Pietrokovski, P. Bork, T. K. Attwood and L. Hood, Gene families: the taxonomy of protein paralogs and chimeras, *Science*, 1997, **278**, 609–614.
29 A. Lewit-Bentley and S. Rety, EF-hand calcium-binding proteins, *Curr. Opin. Struct. Biol.*, 2000, **10**, 637–643.
30 K. G. Kolobynina, V. V. Solovyova, K. Levay, A. A. Rizvanov and V. Z. Slepak, Emerging roles of the single EF-hand Ca^{2+} sensor tescalcin in the regulation of gene expression, cell growth and differentiation, *J. Cell Sci.*, 2016, **129**, 3533–3540.
31 J. Jia, S. Tarabykina, C. Hansen, M. Berchtold and M. Cygler, Structure of apoptosis-linked protein ALG-2: insights into Ca^{2+}-induced changes in penta-EF-hand proteins, *Structure*, 2001, **9**, 267–275.
32 M. Ikura, Calcium binding and conformational response in EF-hand proteins, *Trends Biochem. Sci.*, 1996, **21**, 14–17.
33 N. D. Rawlings and A. J. Barrett, Evolutionary families of metallopeptidases, *Methods Enzymol.*, 1995, **248**, 183–228.
34 M. A. Holmes and B. W. Matthews, Structure of thermolysin refined at 1.6 A resolution, *J. Mol. Biol.*, 1982, **160**, 623–639.
35 C. A. Smith, H. S. Toogood, H. M. Baker, R. M. Daniel and E. N. Baker, Calcium-mediated thermostability in the subtilisin superfamily: the crystal structure of Bacillus Ak.1 protease at 1.8 A resolution, *J. Mol. Biol.*, 1999, **294**, 1027–1040.
36 J. Gu, Y. Feng, X. Feng, C. Sun, L. Lei, W. Ding, F. Niu, L. Jiao, M. Yang, Y. Li, X. Liu, J. Song, Z. Cui, D. Han, C. Du, Y. Yang, S. Ouyang, Z. J. Liu and W. Han, Structural and biochemical characterization reveals LysGH15 as an unprecedented "EF-hand-like" calcium-binding phage lysin, *PLoS Pathog.*, 2014, **10**, e1004109.
37 M. Sanz-Gaitero, R. Keary, C. Garcia-Doval, A. Coffey and M. J. van Raaij, Crystal structure of the lytic CHAP(K) domain of the endolysin LysK from Staphylococcus aureus bacteriophage K, *Virol. J.*, 2014, **11**, 133.
38 E. A. Permyakov, *Metal binding proteins: structure, properties, and functions*, Scientific World, Moscow, 2012.
39 H. E. Jones, I. B. Holland and A. K. Campbell, Direct measurement of free Ca(2+) shows different regulation of Ca(2+) between the periplasm and the cytosol of Escherichia coli, *Cell Calcium*, 2002, **32**, 183–192.
40 R. Young, Phage lysis: do we have the hole story yet?, *Curr. Opin. Microbiol.*, 2013, **16**, 790–797.
41 M. Rajaure, J. Berry, R. Kongari, J. Cahill and R. Young, Membrane fusion during phage lysis, *Proc. Natl. Acad. Sci. U. S. A.*, 2015, **112**, 5497–5502.
42 S. H. Moussa, V. Kuznetsov, T. A. Tran, J. C. Sacchettini and R. Young, Protein determinants of phage T4 lysis inhibition, *Protein Sci.*, 2012, **21**, 571–582.
43 E. Ramanculov and R. Young, Genetic analysis of the T4 holin: timing and topology, *Gene*, 2001, **265**, 25–36.
44 R. White, S. Chiba, T. Pang, J. S. Dewey, C. G. Savva, A. Holzenburg, K. Pogliano and R. Young, Holin triggering in real time, *Proc. Natl. Acad. Sci. U. S. A.*, 2011, **108**, 798–803.
45 R. Young, Phage lysis: three steps, three choices, one outcome, *J. Microbiol.*, 2014, **52**, 243–258.
46 G. V. Mikoulinskaia, S. V. Chernyshov, M. S. Shavrina, N. V. Molochkov, V. Y. Lysanskaya and A. A. Zimin, Two novel thermally resistant endolysins encoded by pseudo T-even bacteriophages RB43 and RB49, *J. Gen. Virol.*, 2018, **99**, 402–415.